

## Supporting Information

### **Novel BiOI/LaOXI<IX> heterojunction with enhanced visible-light driven photocatalytic performance: interlayer electron transition and mechanism unveiling**

**Mengshi Zhou,<sup>1</sup> Chunxiao Zhang,<sup>1,2,a)</sup> Chaoyu He,<sup>1</sup> Jin Li,<sup>1</sup> Tao Ouyang,<sup>1</sup> Chao Tang,<sup>1,a)</sup> and Jianxin Zhong<sup>1</sup>**

1 Hunan Key Laboratory for Micro-Nano Energy Materials and Devices, Laboratory for Quantum Engineering and Micro-Nano Energy Technology, School of Physics and Optoelectronics, Xiangtan University, Hunan 411105, People's Republic of China

2 School of Physics and Optoelectronic Engineering, Shandong University of Technology, Zibo, Shandong 255100, People's Republic of China

a) Authors to whom correspondence should be addressed:

zhangchunxiao@sdut.edu.cn, Tel.: +86 731 58292195 and tang\_chao@xtu.edu.cn,  
Tel.: +86 731 58292437.

**Table S1.** The system (lattice mismatch), stacking types, lattice parameters ( $a, b$ ), binding energies ( $E_b$ ), band gap ( $E_{\text{gap}}$ ) and band type of BiOI-LaOXI heterojunctions in PBE functional.

System (lattice mismatch)	Stacking types	$a(\text{\AA})$	$b(\text{\AA})$	$E_b(\text{eV})$	$E_{\text{gap}}(\text{eV})$	Band type
	AA	3.99	3.99	-0.90303	0.429	d(II)
BiOI/LaOFI	AB	4.01	4.01	-1.049035	-0.0672	Metallic
<IF>	AC	4.12	4.02	-1.373715	0.4943	d(II)
BiOI-LaOFI	AD	3.99	4.01	-0.971248	0.119	d(II)
0.16%	AA	3.99	3.99	-0.852538	1.5577	i(I)
BiOI/LaOFI	AB	4.00	4.00	-0.967281	1.443	i(I)
<II>	AC	4.10	3.99	-1.184994	1.3457	i(I)
	AD	3.99	4.00	-0.898098	1.5532	i(I)
	AA	4.03	4.03	-0.145515	1.4646	d(II)
BiOI/LaOCII	AB	4.05	4.05	-0.310075	0.9597	d(II)
<ICl>	AC	4.04	4.03	-0.200403	1.3678	d(II)
BiOI-LaOCII	AD	4.03	4.04	-0.200019	1.3816	d(II)
1.64%	AA	4.04	4.04	-0.148694	1.4672	i(I)
BiOI/LaOCII	AB	4.04	4.04	-0.269517	1.4562	i(I)
<II>	AC	4.04	4.03	-0.195731	1.4595	i(I)
	AD	4.03	4.04	-0.195761	1.4703	i(I)
	AA	4.05	4.05	-0.135011	1.4467	i(I)
BiOI/LaOBrI	AB	4.06	4.06	-0.278529	1.3674	d(II)
<IBr>	AC	4.05	4.05	-0.185585	1.431	i(I)
BiOI-LaOBrI	AD	4.05	4.05	-0.185082	1.4537	i(I)
2.29%	AA	4.05	4.05	-0.137434	1.4362	i(I)
BiOI/LaOBrI	AB	4.05	4.05	-0.259983	1.4293	i(I)
<II>	AC	4.05	4.05	-0.184387	1.4304	i(I)
	AD	4.05	4.05	-0.184885	1.4486	i(I)

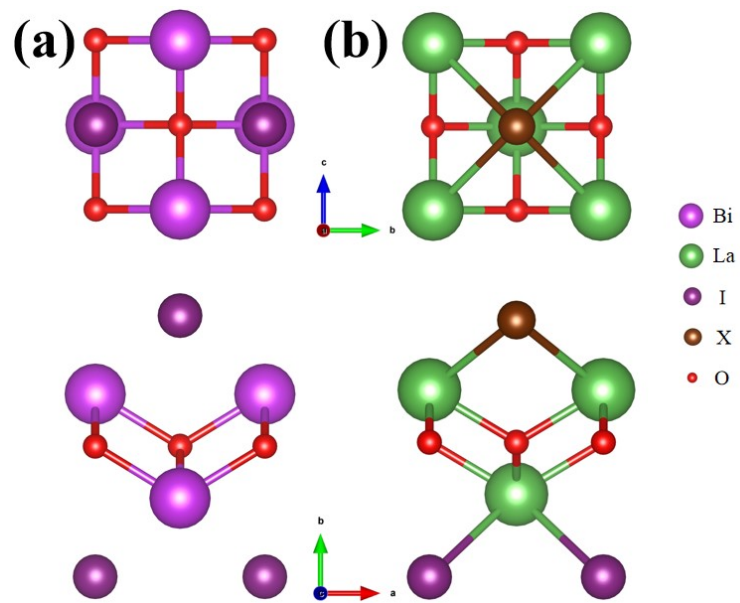


Figure S1. The top and side view of monolayer structure of (a) BiOI and (b) LaOXI.

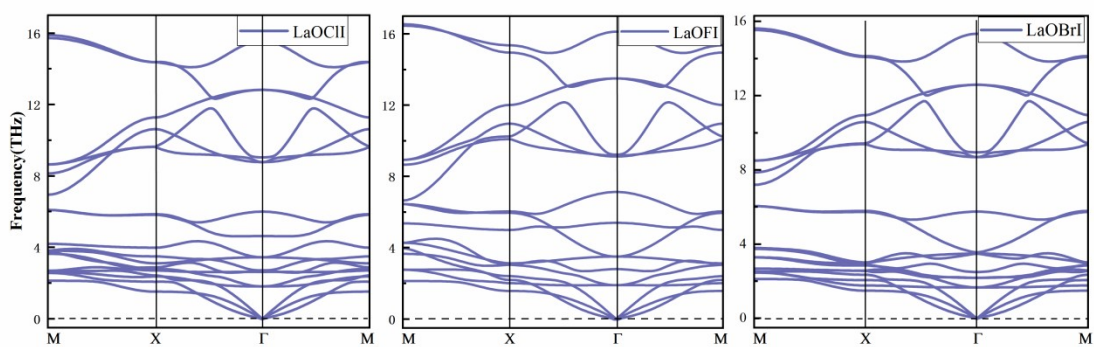


Figure S2. Phonon dispersion curve for monolayer (a) LaOCII, (b) LaOFI and (c) LaOBrI.

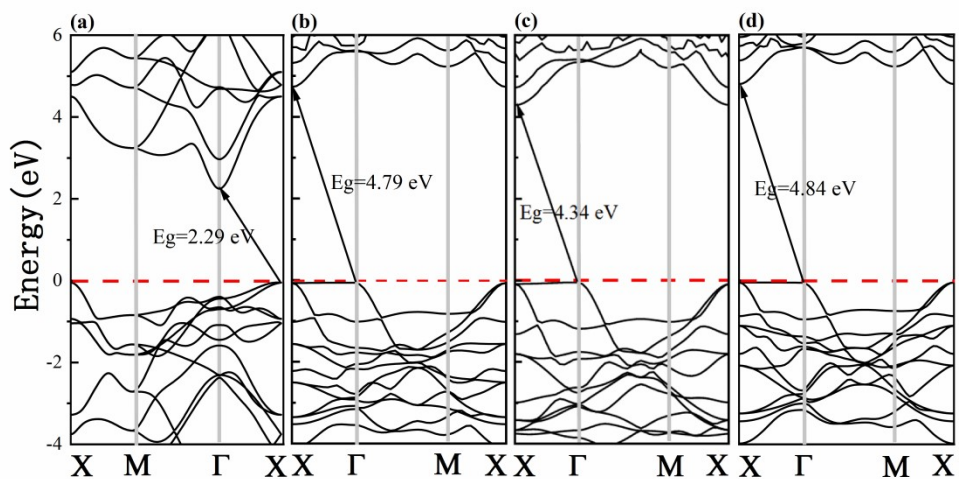


Figure S3. The bandstructure of monolayer for (a) BiOI, (b) LaOClI, (c) LaOFI and (d) LaOBrI.

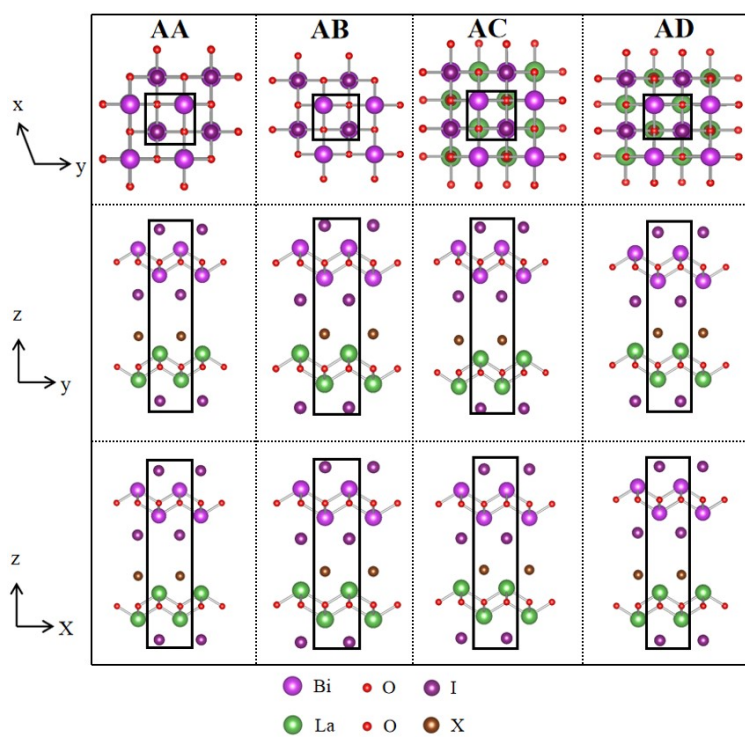


Figure S4. The top and side view of four stacks of heterostructures of BiOI-LaOXI.

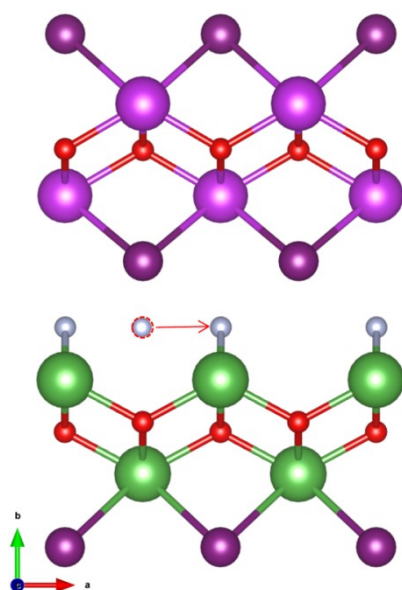


Figure S5. The optimized BiOI/LaOFI<IF> heterojunction with structural distortion from the side view. The red dashed circle indicates the original position of the F atom.

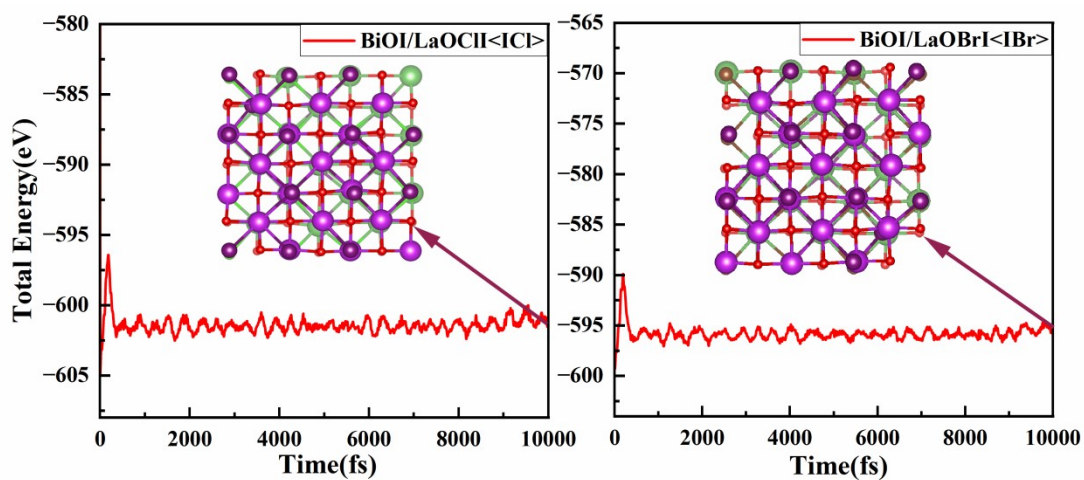


Figure S6 Evolution of total energies per atom of AB-BiOI/LaOCII<ICl> and AB-BiOI/LaOBrI<IBr> heterojunctions with 3×3 supercells obtained from 10 ps AIMD simulations. The final conformations at  $t = 10$  ps are shown in the insets.



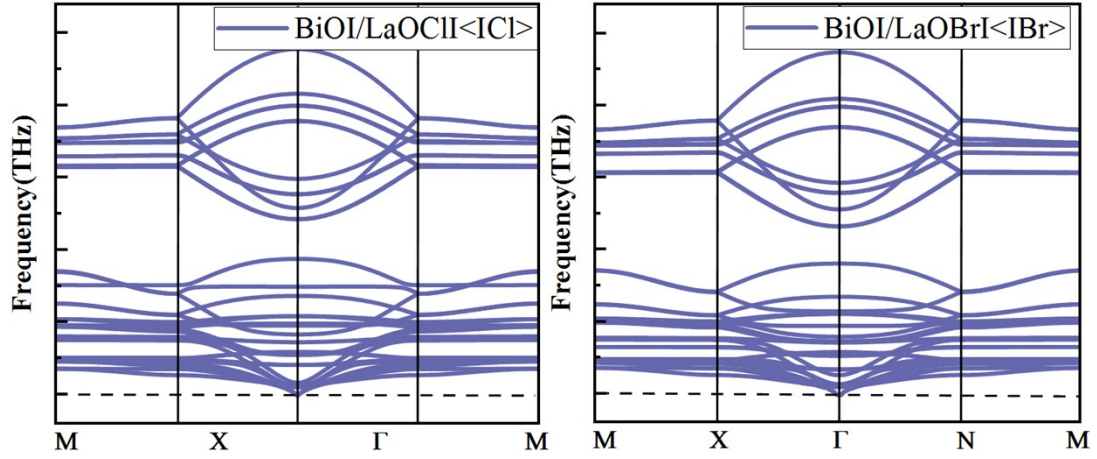


Figure S7. Phonon dispersion spectrum of AB-BiOI/LaOCII<ICI> and AB-BiOI/LaOBrI<IBr> heterojunctions.

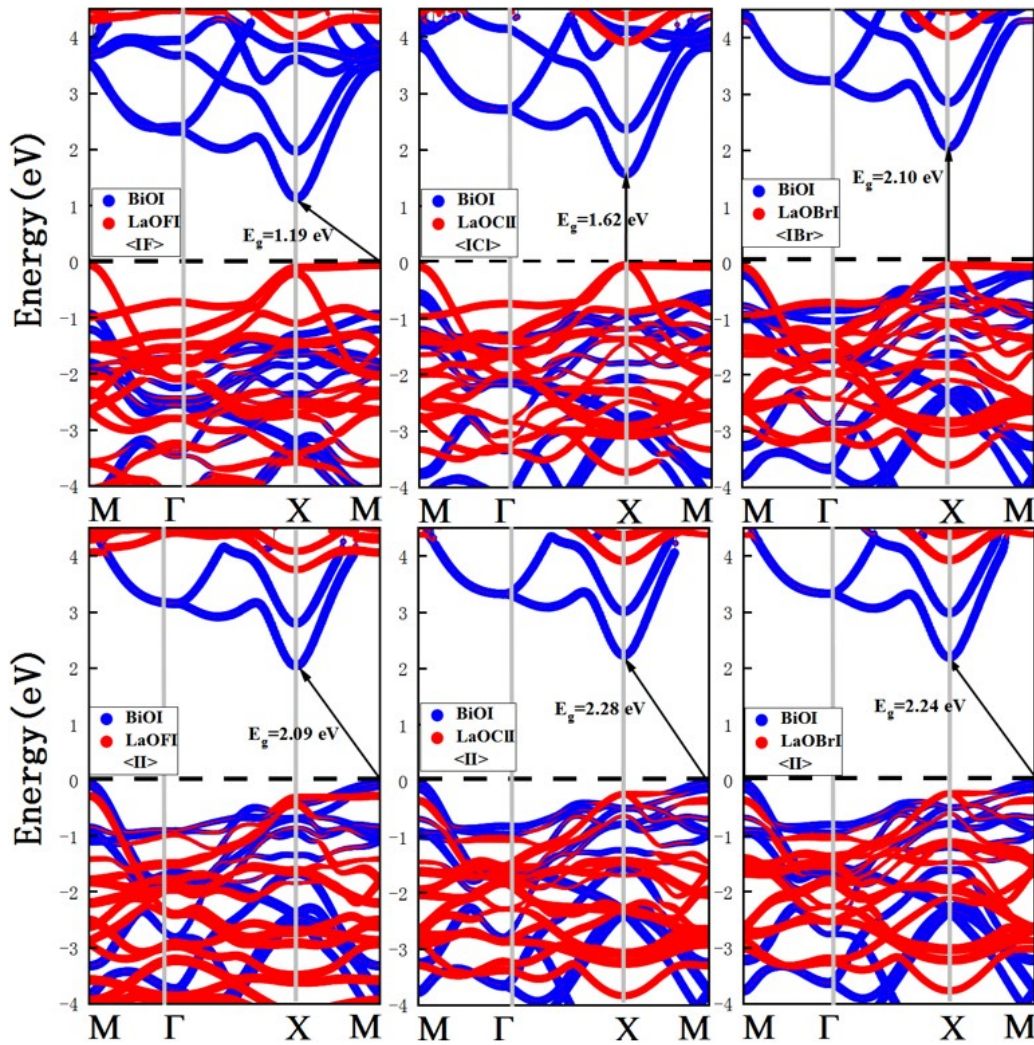


Figure S8. Projected band structures of BiOI-LaOXI<IX> heterostructures with the most stable stack using the HSE06 functional.

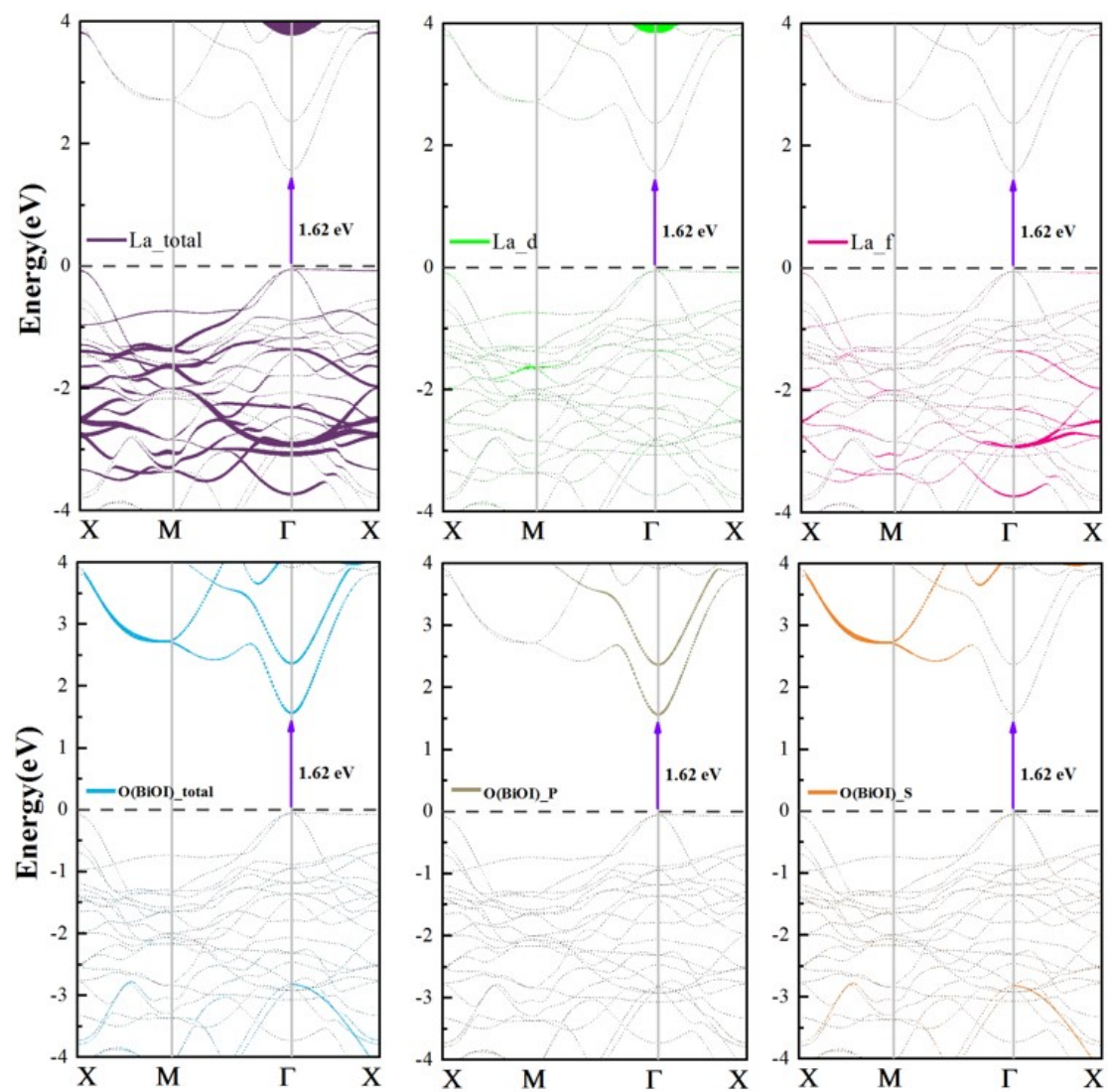


Figure S9. The projected bands of the BiOI/LaOCl $\langle ICI \rangle$  vdW heterostructure are contributed to by the masked La $_d$  and f orbitals, as well as the BiOI O orbitals.

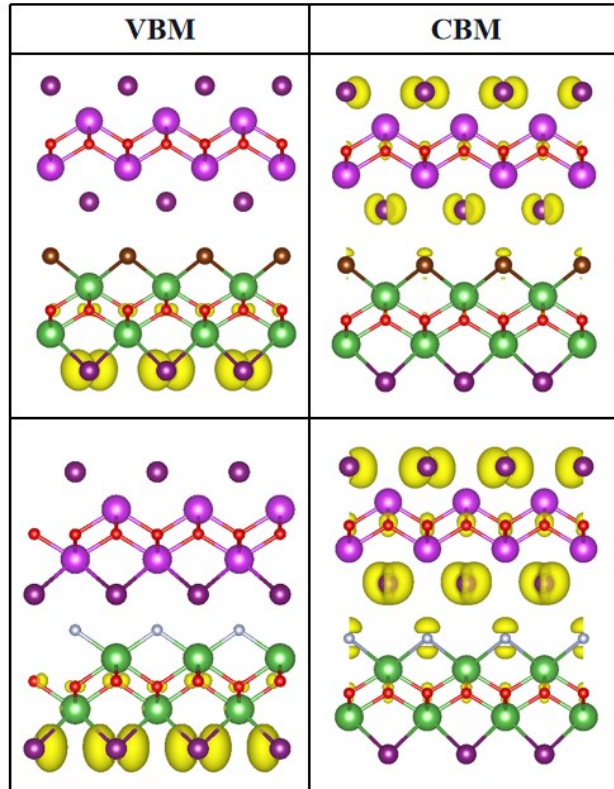


Figure S10. Band decomposed charge density of CBM and VBM for BiOI/LaOBr<IBr> and BiOI/LaOFI<IF>.



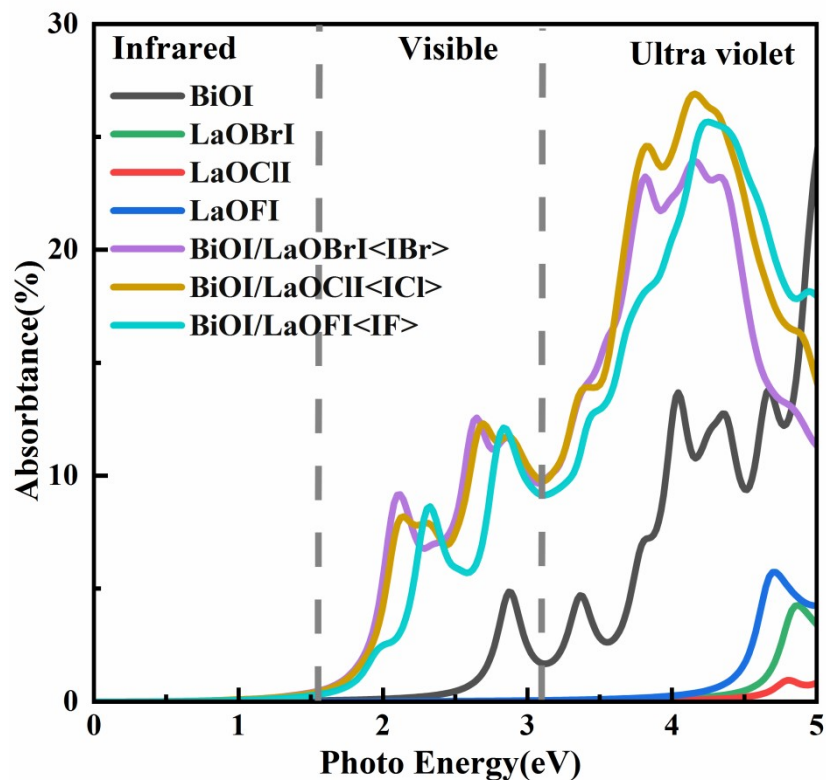


Figure S11. The optical absorbance of isolated BiOI, LaOCII, LaOFI and BiOI/LaOXI<IX> vdW heterostructures, respectively.

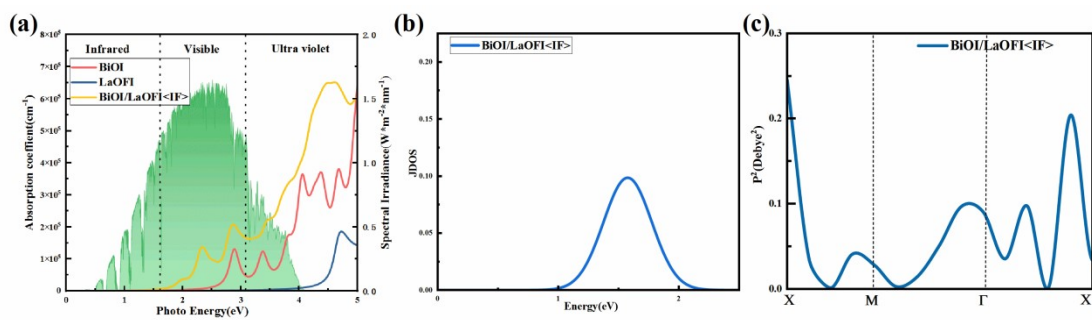


Figure S12. The optical absorbance of isolated BiOI, LaOFI and BiOI/LaOFI<IF> vdW heterostructure, respectively.

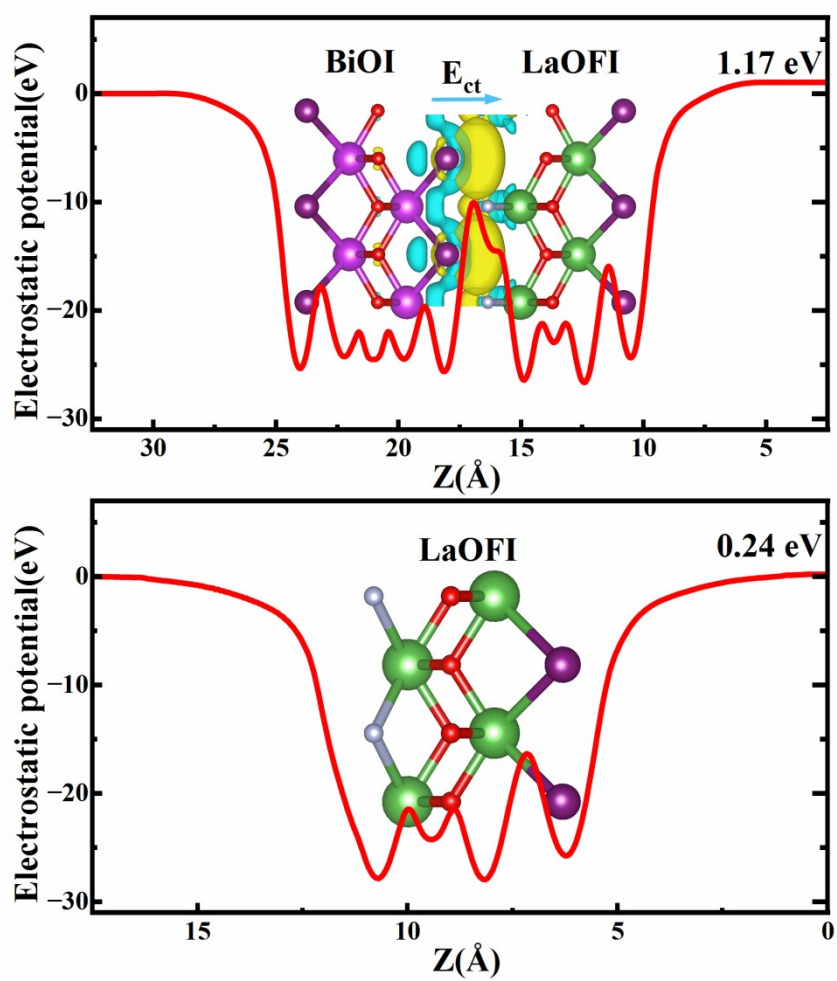


Figure S13. The electrostatic potential of heterostructure BiOI/LaOFI<IF> and monolayer LaOFI. The plot inserted in the one above shows the charge density difference along  $z$  axis.

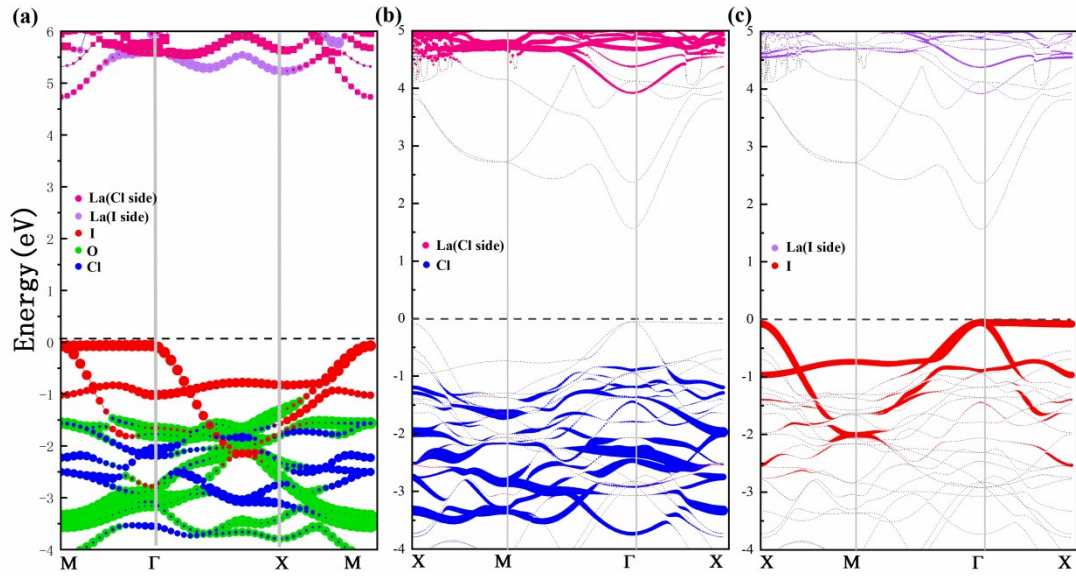


Figure S14. (a) Projected band of the LaOClI; (b) and (c) depict La-Cl and La-I resolved projected bands in the BiOI/LaOClI<ICl>.

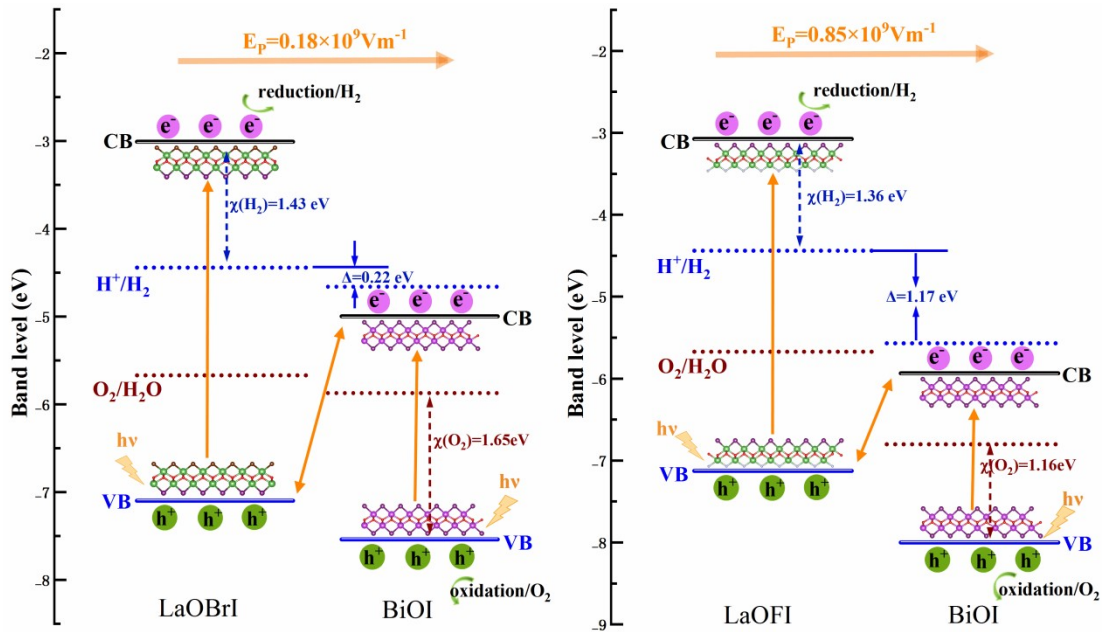


Figure S15. Band alignments of BiOI/LaOBrI<IBr> and BiOI/LaOFI<IF> based on the SHE model.

## Calculation of Dipole Moment

The dipole moment could be obtained from the output file OUTCAR. The unit of dipole moment in OUTCAR is “e·Å”. The unit conversion between “e·Å” and “Debye” is as follows:  $1 \text{ e}\cdot\text{\AA} = 4.80 \text{ Debye}$ .

The unit of dipole moment used for polarized electric field calculations is Coulomb meter (C·m). The unit conversion between “e·Å” and “C·m” is as follows:  $1 \text{ e}\cdot\text{\AA} = 1.602176634 \times 10^{-29} \text{ C}\cdot\text{m}$ .

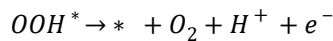
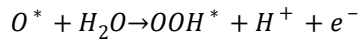
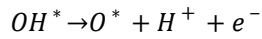
## Free Energy Difference ( $\Delta G$ )

To compute the free energy difference ( $\Delta G$ ) in the water redox reactions, we adopted the method developed by Nørskov et al<sup>77</sup>, according to which the  $\Delta G$  of an electrochemical reaction is computed as :

$$\Delta G = \Delta E + \Delta E_{ZPE} - T\Delta S + \Delta G_U$$

where  $\Delta E$  is the adsorption energy, and  $\Delta E_{ZPE}$  and  $\Delta S$  are the difference in zero point energy and entropy difference between the adsorbed state and the gas phase, respectively.  $T$  is the system temperature (298.15 K, in our work).  $\Delta G_U$  represents the contribution of photogenerated electrode potential ( $U_e / U_h$ ) to  $\Delta G$ , which is relative to the normal hydrogen electrode (NHE). For those reactions involving the release of protons and electrons, the free energy of one pair of proton and electron ( $H^+ + e^-$ ) was taken as  $1/2G_{H_2}$ . The free energy of  $O_2(g)$  was derived as  $G_{O_2} = 2G_{H_2O} - 2G_{H_2} + 4.92$  eV since  $O_2$  in triplet ground state is notoriously poorly described by DFT calculations.

There are four steps to transform  $H_2O$  into  $O_2$  molecule in oxidation half reaction, which can be written as:



where  $*$  is the active site on photocatalysts,  $O^*$ ,  $OH^*$ , and  $OOH^*$  represent the adsorbed intermediates.

For each reaction of both oxidation and hydrogen production, the free energy difference under an extra potential bias can be written as:

$$\Delta G_1 = G_{OH^*} + \frac{1}{2}G_{H_2} - G_* - G_{H_2O} + \Delta G_U$$

$$\Delta G_2 = G_{O^*} + \frac{1}{2}G_{H_2} - G_{OH^*} + \Delta G_U$$

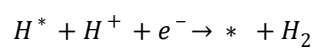
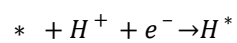
$$\Delta G_3 = G_{OOH^*} + \frac{1}{2}G_{H_2} - G_{O^*} - G_{H_2O} + \Delta G_U$$

$$\Delta G_4 = G_* + \frac{1}{2}G_{H_2} - G_{O_2} - G_{OOH^*} + \Delta G_U$$

$\Delta G_U$  ( $\Delta G_U = -eU$ ) denotes extra potential bias provided by an electron in the electrode, where  $U$  is the electrode potential relative to the standard hydrogen electrode (SHE).



The hydrogen production half reaction with two-electron pathways, can be written as:



where \* is the active site on photocatalysts, O\*, OH\*, OOH\* and H\* represent the adsorbed intermediates.

### References

1. J. K. Nørskov, J. Rossmeisl, A. Logadottir, L. Lindqvist, J. R. Kitchin, T. Bligaard and H. Jónsson, *The Journal of Physical Chemistry B*, 2004, **108**, 17886-17892.